Int J Clin Exp Med 2018;11(12):12956-12963
www.ijcem.com /ISSN:1940-5901/IJCEM0071406

Original Article

Stress and stability of newly designed medial anatomic locking plates and traditional fixations in the treatment of posterointernal tibial plateau fracture: a comparative finite element study

Fancheng Chen[1*], Silin Wu[2*], Zeyuan Zhong[1*], Xiaowei Huang[3], Rongguang Ao[1], Xv Zhang[1], Dejian Li[1], Zhi Qian[1], Xiaobiao Zhang[2], Baoqing Yu[4]

[1]Shanghai Medical College, Fudan University, Shanghai, China; [2]Department of Neurosurgery, Zhongshan Hospital, Fudan University, Shanghai, China; [3]Department of Orthopedics, First Affiliated Hospital of Suzhou University, Jiangsu, China; [4]Department of Orthopedics, Shanghai Pudong Hospital, Fudan University Pudong Medical Center, Shanghai, China. [*]Equal contributors.

Received December 22, 2017; Accepted June 1, 2018; Epub December 15, 2018; Published December 30, 2018

Abstract: Purpose: This study aimed to analyze the biomechanical stability of a new designed plate for posterointernal tibial plateau fracture fixation, and compare with traditional fixation implants, including cancellous screws and a L-shape locking plate. Methods: A posterointernal tibial plateau fracture three-dimensional (3D) model was reconstructed by finite element analysis (FEA) software. A 400 N axis load was created with a 60% distribution on the medial tibial plateau surface, while the distal end of tibia was fully fixed, to simulate the bipedal static stance. Equivalent von Mises stress (EVMS), displacement and equivalent maps of displacement and stress of the models fixed by different fixations were output for comparison. Results: The maximal stress of the cancellous screw group, the L-shape locking plate group and the newly designed plate group was 4.4178 MPa, 9.7438 MPa and 20.1355 MPa, respectively. Peak displacement of three groups was all less than 2 mm which was usually to evaluate whether reduction of the fracture was successful. Conclusions: This study illustrates that newly designed anatomic locking plates have superior performance in posterointernal tibial plateau fracture fixation and serve as a suitable clinical alternative fixation method.

Keywords: Finite element analysis, posterointernal tibia plateau fracture, comparison

Introduction

Tibial plateau fracture is a common fracture, accounting for approximately 10% of lower limb fractures and 1% of all fractures in adults, due to high-energy trauma [1]. Rigid anatomical reduction is necessary for treating this kind of fracture to avoid severe complications, such as infection and osteoarthritis [2, 3]. The 2 most common fixations to maintain the fractured tibial plateau are screws fixations and locking plate fixation [4]. However, both of them have disadvantages for clinical use. Fixation with screws is easy to loosen and the locking plate fixation has the risk of fixation failure [5].

In this study, a new medial locking plate was designed for possessing better stability of the posterointernal tibial plateau fracture fixation. The shape of the plate, which could fit the concavity below the medial tibial plateau of Chinese patients, designed by seasoned orthopedic surgeons. Furthermore, it was shown in a recent study that crossed screws provide better fixation than parallel screws [6]. As a result, the universal holes were designed as the proximal screw holes which allowed to choose the best direction of screws for bone fragments fixation during the operation. Moreover, there is an elliptical hole was positioned in the middle of the plate for adjusting the degrees of plate in surgery. In addition, three Kirschner's wire holes located at the proximal edge of the plate were included for temporary fixation. Although the newly designed plate already was patented and achieved a satisfactory clinical outcome, the biomechanism of new plate had not yet been compared computationally with traditional implants.

Finite element analysis (FEA) is a computational technology for calculating the mechanics

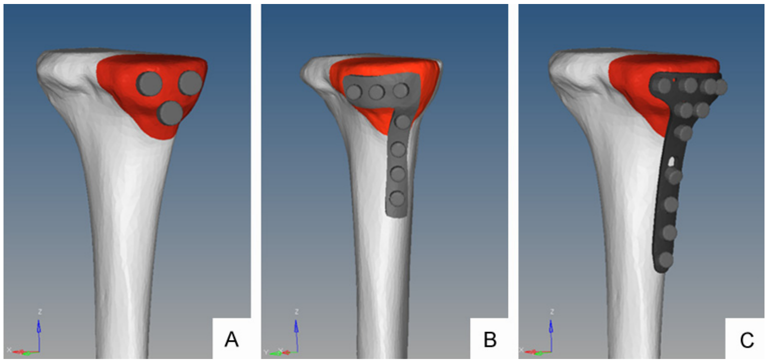

Figure 1. Three models after implants assemblage (A) Model A which fixed by three cancellous screws. (B) Model B which fixed by L-shape plate. (C) Model C which fixed by new designed plate.

Table 1. Number of nodes and elements in each model

Variable	Elements	Nodes
Model A	116931	22673
Model B	185367	35465
Model C	201725	45099

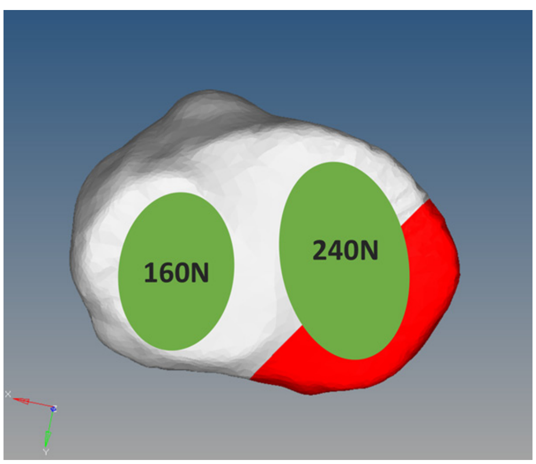

Figure 2. Distribution of 400 N axis compression on the tibial plateau articular surface.

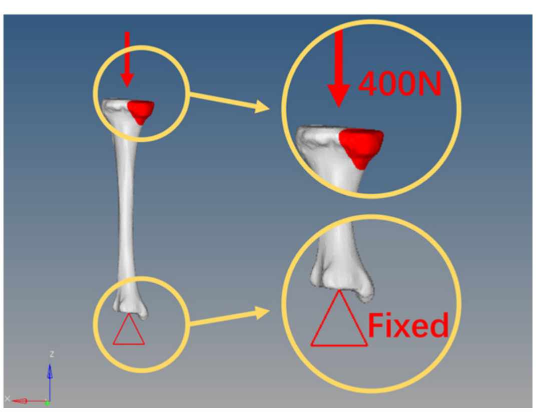

Figure 3. 400 N axis compression of load and constraint at the distal tibia of model to simulate the physiological stress in the bipedal static stance of an adult who weighed 80 kg.

parameter and distribution map of models which imported to software [7, 8]. FEA is extensively used in clinical medicine analysis, especially orthopedics [9, 10]. FEA provides the load distribution and prediction of fixation preoperative for the surgeon as a reference. In this research study, we constructed fixation models of posterointernal tibial plateau fracture with a new design and traditional implants to study. The hypothesis of our study was that the new designed plate would provide better fixation than a traditional one.

Materials and methods

Experimental model

An intact right tibia model was reconstructed in three-dimensional (3D) geometry format by software Mimics 15.0 (Materialize Company, Leuven, Belgium) based on the Initial 1-mm cuts CT data imported. The data was obtained in the Digital Imaging and Communications in Medicine (DICOM) format from a 42-year-old healthy Chinese male excluded comorbidities such as osteoporosis, osteoarthritis, and fractures. Then, an oblique cut from 6 cm distal below the articular surface of tibial plateau to tibial tubercle was created to simulate the simple split fracture of the medial tibia plateau (AO/OTA type 41-B1.1, Schatzker type IV) by Geomagic Studio Software (3D system Inc., Rock Hill, SC, USA). There was no displacement between the two bone fragments. Moreover, the traditional implants, including plates and screws, were drawn using the software Creo 3.0 (Parametric Technology Corporation, USA) based on the manufacturers' specifications. The diameter of cortical screws and cancellous screws were 4.5 mm and 6.5 mm, respectively, while the thickness of traditional plate was 3 mm. Meanwhile, the newly designed plate was created with the specific angle which fit with the bone shape shown in **Figure 1C**. After polishing in the Geomagic, all of models were imported into Hypermesh software

Table 2. Comparison of the structural average result in the finite element analysis

	Model A	Model B	Model C	*P* value
Stress on plate (MPa)	N/A	2.452 ± 1.929	0.984 ± 0.803	<0.001
Stress on screws (MPa)	0.331 ± 0.485	0.719 ± 0.966	0.416 ± 0.456	<0.001
Stress on triangular fragment (MPa)	0.099 ± 0.105	0.139 ± 0.095	0.080 ± 0.079	<0.001
Stress on main part of tibia (MPa)	0.360 ± 0.418	0.401 ± 0.445	0.337 ± 0.435	<0.001
Displacement of models (sum) (mm)	0.680 ± 0.363	0.949 ± 0.361	1.058 ± 0.415	<0.001

Figure 4. Displacement of implants in three models (A) Model A which fixed by three cancellous screws. (B) Model B which fixed by L-shape plate. (C) Model C which fixed by new designed plate.

(v12.5, Altair Engineering Inc., Michigan, USA) to accomplish the installation. Screws fixation, traditional L-shape plate fixation, and newly designed fixation were divided into model A, B, and C, respectively. Model C was comprised of 11 cortical screws, while model B was 7. Meanwhile, 4 proximal screws and 3 distal screws in model C and all screws in model A and B were parallel to the joint surface while other screws in model C were kept at 15° or 30° degrees. Finally, models were tetrameshed into eight-node hexahedron three-dimensional element which will perform better in geometric non-linear analysis than other type of elements. The nodes and elements numbers of each groups are listed in **Table 1**.

Material properties and boundary conditions

The properties of titanium alloy were set as properties of screw and plate models with an elastic modulus of 110 GPa and a Poisson ratio of 0.3 in our research. Additionally, the elastic modulus of 17 and 5 GPa were assigned to cortical bone and the trabecular bone, respectively, with a same Poisson ratio of 0.3 [11]. It's the precondition of our study that all of models including cortical bone, trabecular bone, and implants be assumed to be homogeneous, linear, and elastic materials. Furthermore, the frictional coefficient assumed between the contact surface of bone and screws was 0.3, the coefficient between bone and plate was 0.1, and the frictional coefficient was set as 0.9 between screws and plate to simulate the locking condition of models. Subsequently, a 400 N axis force was pressed the articular surface of tibia model with a distribution to mimic the bipedal static stance of a patient who is weight 80 kg [2], while 60% of the load was distributed

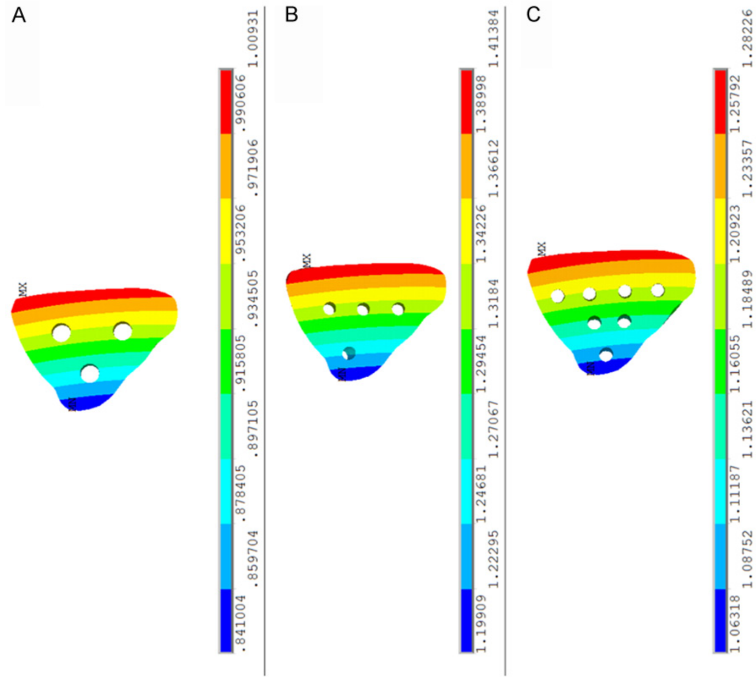

Figure 5. Displacement of three groups on triangular fragment (A) Model A which fixed by three cancellous screws. (B) Model B which fixed by L-shape plate. (C) Model C which fixed by new designed plate.

to the medial part of articular surface (**Figure 2**) [12]. The bottom of the tibia was fully constrained with no displacement (**Figure 3**).

Analysis

After import into ANSYS software, three models were analyzed. The results of each model were output in this study, including the equivalent von Mises Stress (EVMS), displacement and equivalent maps of EVMS, and displacement. Statistical analysis of the results was performed by student t test for comparing whether have statistically significant among three models. A *P* value less than 0.05 was assumed as statistically significant.

Results

Displacement of models

The maximal displacement of group A, B and C was 1.0118 mm, 1.0309 mm and 1.2852 mm, respectively. The average and three different axes displacement of models are listed in **Table 2**. The displacement distribution map is shown in **Figures 4** and **5**. The displacement distribution of the models, however, matched a similar characteristic that the maximal displacement appeared at the part near the proximal edge of each plate and shown a decreasing tendency from the proximal to the bottom of tibia.

Stresses in the models

There was a considerable difference among stress outcome of three groups. From the equivalent maps of stress of the fracture fixation models, the middle of the screws where the borders of two bone fragments appeared, the von Mises stress (EVMS) concentration of screws in group A and proximal screws in group B and C. Stress concentrated in the distal screws in group B and C located near the interaction part where was in direct contact with plate shown in **Figure 6**. Moreover, all the implants showed a tendency that stress increased gradually from the proximal end to the distal. Besides, peak stress was observed around the distal screw hole in group C, which was 20.1355 MPa, and at the bend part of the L-shaped plate in group B, which was 9.7438 MPa, as shown in **Figures 6-8**. The average stress is listed in the **Table 2** and **Figure 9**.

Stresses in the fracture tibial models

The equivalent maps of stress among three models are compared in **Figure 6**. The maximal stress was also found around the screw hole of bone fragment. However, the maximal stress location of bone fragment had an imperceptible difference between the main part of tibia and triangular fragment. Peak stress concentrations were below the screw hole in the main part of tibia which was 4.4178 MPa, 3.51095 MPa and 2.8782 MPa in group A, B, and C, respectively, and above screw holes in the triangular fragment which was 0.8072 MPa, 1.0129 MPa, and 0.92123 MPa in group A, B, and C, respectively. Additionally, the middle and lower part of tibia were also observed a load concentration.

Discussion

Posterointernal tibial plateau fracture was not uncommon in clinical medicine which was often

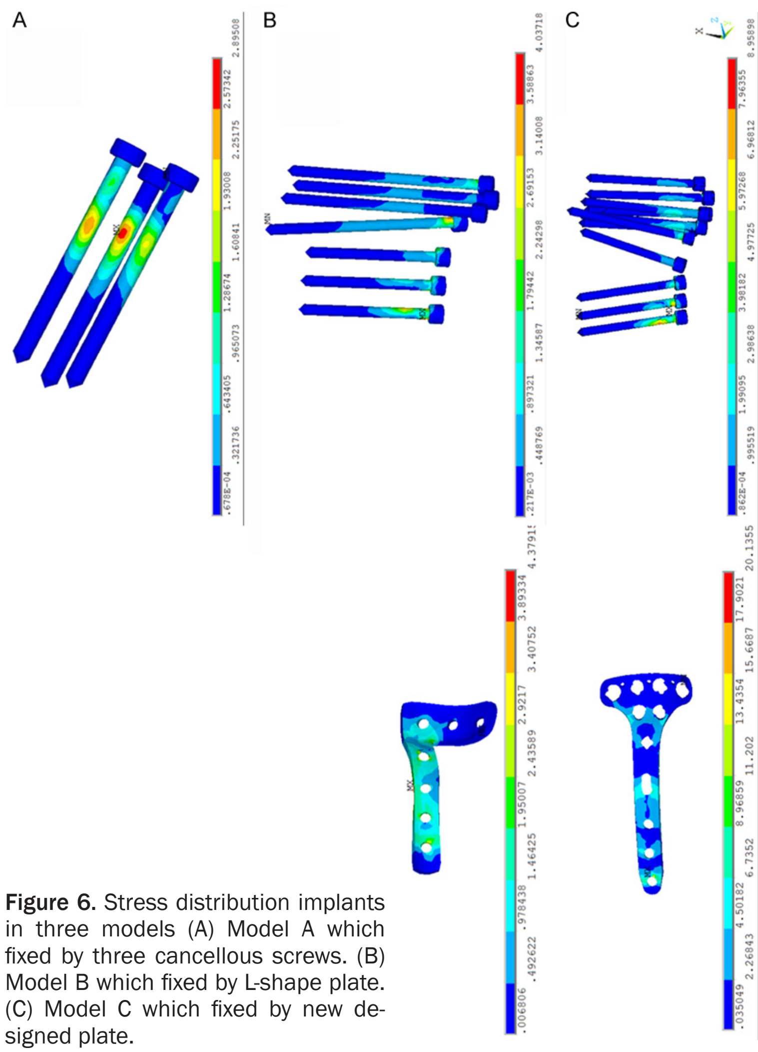

Figure 6. Stress distribution implants in three models (A) Model A which fixed by three cancellous screws. (B) Model B which fixed by L-shape plate. (C) Model C which fixed by new designed plate.

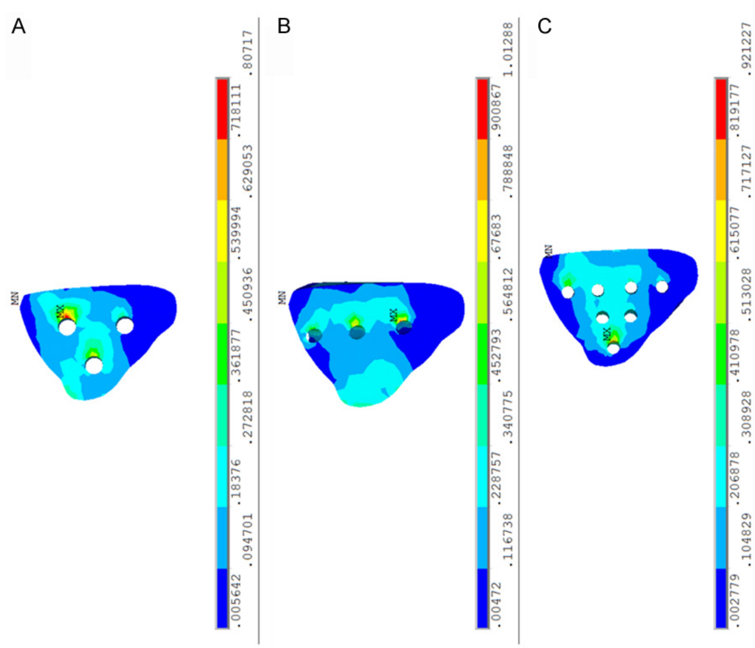

Figure 7. Stress distribution of three models on triangular fragment (A) Model A which fixed by three cancellous screws. (B) Model B which fixed by L-shape plate. (C) Model C which fixed by new designed plate.

due to high-energy trauma, such as bruise, falls from elevations and car accidents [13]. A proper fixation treatment had an important significance for the functional recovery of knee. Currently, cancellous screws fixation and locking plate fixation are the two most frequent methods used in the clinic [3, 14]. However, both of them have disadvantages for fracture fixation, while the screws are easy to loosen, the locking plate has the hazard of breakage. We designed a new locking plate which has been patented and achieved favorable outcomes, and we performed a FEA of models which were fixed by cancellous screws, traditional L-shape plate, and new design plate in this study to verify the biomechanical advantage of new designed locking plate computationally [15].

From the FEA result of three models, the location of stress concentration was shown around the screws holes, especially the distal ones shown in the **Figure 6**. This phenomenon not only appeared in the plate, but the holes of fragments of tibia, which also was mentioned in other biomechanistic studies [9, 16], indicating that the load transmission of compression from articular surface was dispersed by every screw and the plate provided the anti-sliding effect. On the one hand, this finding verified the assignment in this

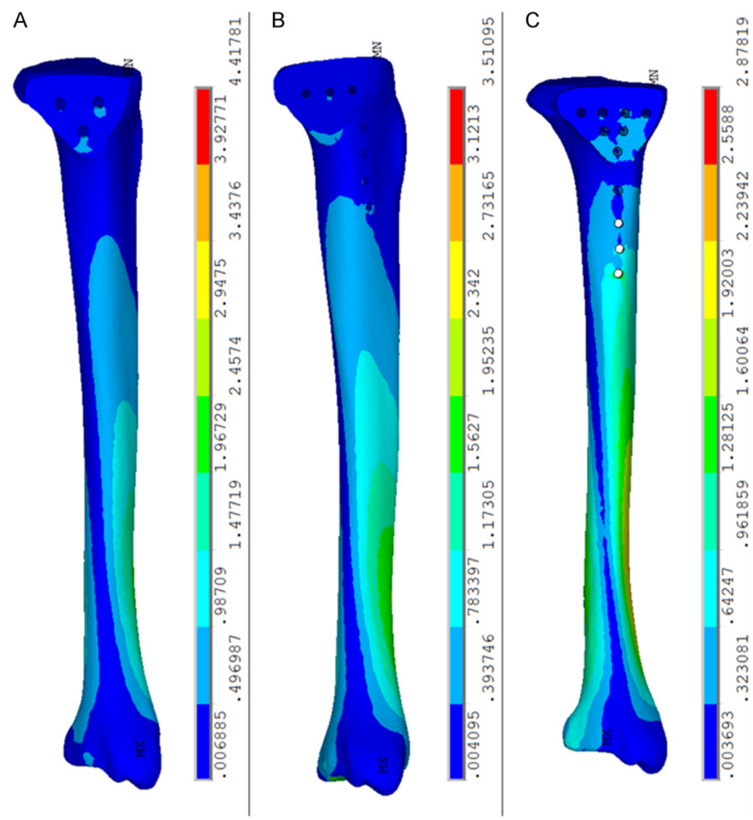

Figure 8. Stress distribution of three models on main part of tibia (A) Model A which fixed by three cancellous screws. (B) Model B which fixed by L-shape plate. (C) Model C which fixed by new designed plate.

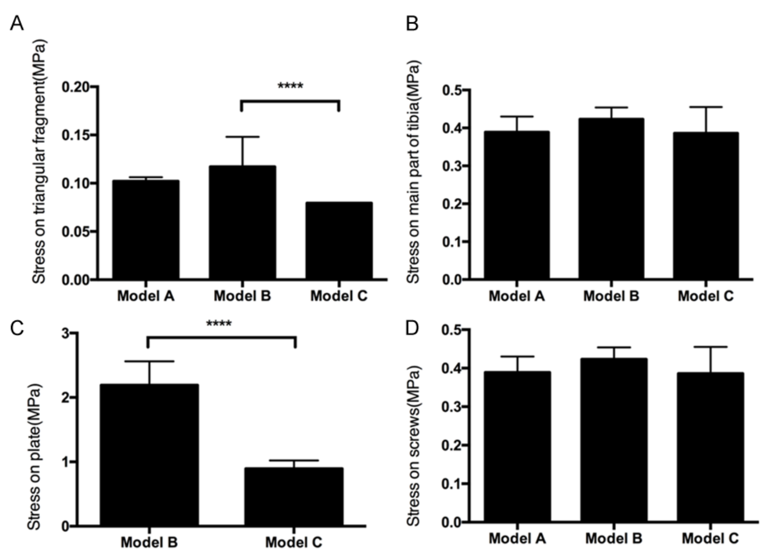

Figure 9. Comparison of mean stress value of two models. ****P<0.001, A. The mean stress on triangular fragment (MPa) after loading. B. Mean stress on main part of tibia (MPa) after loading. C. Mean stress on plate (MPa) after loading. D. Mean stress on screws (MPa) after loading.

study was consistence with other researches. On the other hand, it suggested that the intensity of plate near screw holes should be strengthened for avoiding the failure of implants. Additionally, it was noticed that Von Mises stress was concentrated near the middle of the proximal screw where interacted with fracture line of model directly. This could be understood that the support provided by screws protected the bone fragment from sliding. Moreover, concentration also presented at head of the most distal screw of group B and C where contact with plate directly, implying that the most distal screw had a great significance for buttress. So, the maximal Von Mises stress of group C was 8.9590 MPa which was larger than other two groups, meaning that the screws in group C shared more stress than group A (2.8951 MPa) and B (4.2994 MPa). Otherwise, the stress concentration occurred at the bend of T-shape plate could explained by leverage of load transmitted from the proximal screws.

Additionally, the average stress of all models in triangular fragment was the model C which was only 0.080 MPa, meaning the new designed plate provided a great holding role and shared a large part of stress from articular compression. Moreover, the comparison of average stress of models illustrated that the new designed plate, 0.984 MPa, also was lower than traditional one which was 2.452, indicating the traditional plate might have more possibility of implant breakage comparing with new one in same condition.

Interestingly, it was observed that the lower anterior part of three tibial models showed a stress concentration which, could be explained by the specific slender outline of tibia, and which was also found in other tibial biomechanical research [17, 18]. This indicates that the models we created for mimicking the tibia could basically reflect the real situation of tibia. Furthermore, stress-relaxing zones was found between two adjoining screw hole of main part tibia which indicated that the plate provided a rigid buttress because of the shielding effect due to the difference of elastic modulus between the material of bone and plate [19].

The displacement of models after compression of load was also calculated in this study. As reported in other study, 2 mm of displacement was regarded as a watershed issues to evaluate whether the reduction was a success [11, 20]. The peak displacement of all three models in this study, however, was below the threshold, implying that all of three methods mentioned in this research could perform well in bipedal static stance after surgery.

There are still several limitations in this study. First, the cortical and cancellous bone was assigned as homogeneous, linear and elastic materials which had an imperceptible difference from the reality situation. Second, the trades of screws and the fibula were neglected to simplify the models for improving the success ratio of convergence, which also was not consistent with real conditions. Third, cyclic loading for simulating the dynamic joint motion had not been performed in this study which required superior computer resources and complex calculating strategy. Thus, the displacement results in this study might be lower than reality.

Conclusion

Our newly designed locking plate performed well in comparison with the traditional fixations which could provide satisfactory fixation in clinical surgery. Additionally, the long-term effect of this plate still needed to be studied in the further research.

Acknowledgements

I want to take this chance to thank Jinlong Liu, a professor of Shanghai Children's Medical Center, and his research group for their contribution to this research. The key specialty medical program of Shanghai Municipal Commission of Health and Family Planning, Award Number: ZK2015B17; The Outstanding Leaders Training Program of Pudong Health Bureau of Shanghai, Award Number: PWR12013-01; Foundation of Ministry of Science and Technology of People's Republic of China, Award Number: 2016YFC-0106103.

Disclosure of conflict of interest

None.

Abbreviations

EVMS, von Mises Stress; DICOM, Digital Imaging and Communications in Medicine; FEA, Finite element analysis.

Address correspondence to: Baoqing Yu, Department of Orthopedics, Shanghai Pudong Hospital, Fudan University Pudong Medical Center, 2800 Gongwei Road, Huinan Town, Pudong New Area, Shanghai, China. Tel: +8618017395772; E-mail: doctorbqy@126.com

References

[1] Moore TM, Patzakis MJ, Harvey JP. Tibial plateau fractures: definition, demographics, treatment rationale, and long-term results of closed traction management or operative reduction. J Orthop Trauma 1987; 1: 97-119.

[2] Carrera I, Gelber PE, Chary G, González-Ballester MA, Monllau JC, Noailly J. Fixation of a split fracture of the lateral tibial plateau with a locking screw plate instead of cannulated screws would allow early weight bearing: a computational exploration. Int Orthop 2016; 40: 2163-2169.

[3] McNamara IR, Smith TO, Shepherd KL, Clark AB, Nielsen DM, Donell S, Hing CB. Surgical fixation methods for tibial plateau fractures. Cochrane Database Syst Rev 2015; 15: CD009679.

[4] Rademakers MV, Kerkhoffs GM, Sierevelt IN, Raaymakers EL, Marti RK. Operative treatment of 109 tibial plateau fractures: five- to 27-year follow-up results. J Orthop Trauma 2007; 21: 5-10.

[5] Phisitkul P, McKinley TO, Nepola JV, Marsh JL. Complications of locking plate fixation in complex proximal tibia injuries. J Orthop Trauma 2007; 21: 83-91.

[6] Yao F, He Y, Qian H, Zhou D, Li Q. Comparison of biomechanical characteristics and pelvic ring stability using different fixation methods to treat pubic symphysis diastasis: a finite element study. Medicine (Baltimore) 2015; 94: e2207.

[7] Geramy A, Bouserhal J, Martin D, Baghaeian P. Bone stress and strain modification in diastema closure: 3D analysis using finite element method. Int Orthod 2015; 13: 274-86.
[8] Hu XJ, Wang H. Biomechanical assessment and 3D finite element analysis of the treatment of tibial fractures using minimally invasive percutaneous plates. Exp Ther Med 2017; 14: 1692-1698.
[9] Zhang YK, Wei HW, Lin KP, Chen WC, Tsai CL, Lin KJ. Biomechanical effect of the configuration of screw hole style on locking plate fixation in proximal humerus fracture with a simulated gap: a finite element analysis. Injury 2016; 47: 1191-5.
[10] Liu GT, Balldin BC, Zide JR, Chen CT. A biomechanical analysis of interference screw versus bone tunnel fixation of flexor hallucis longus tendon transfers to the calcaneus. J Foot Ankle Surg 2017; 56: 813-816.
[11] Chen P, Lu H, Shen H, Wang W, Ni B, Chen J. Newly designed anterolateral and posterolateral locking anatomic plates for lateral tibial plateau fractures: a finite element study. J Orthop Surg Res 2017; 12: 35.
[12] Huang X, Zhi Z, Yu B, Chen F. Stress and stability of plate-screw fixation and screw fixation in the treatment of schatzker type IV medial tibial plateau fracture: a comparative finite element study. J Orthop Surg Res 2015; 10: 182.
[13] Yu L, Fenglin Z. High-energy tibial plateau fractures: external fixation versus plate fixation. Eur J Orthop Surg Traumatol 2015; 25: 411-423.
[14] Conserva V, Vicenti G, Allegretti G, Filipponi M, Monno A, Picca G, Moretti B. Retrospective review of tibial plateau fractures treated by two methods without staging. Injury 2015; 46: 1951-1956.
[15] van Dreumel RL, van Wunnik BP, Janssen L, Simons PC, Janzing HM. Mid- to long-term functional outcome after open reduction and internal fixation of tibial plateau fractures. Injury 2015; 46: 1608-1612.
[16] Ramlee MH, Kadir MR, Murali MR, Kamarul T. Finite element analysis of three commonly used external fixation devices for treating type III pilon fractures. Med Eng Phys 2014; 36: 1322-1330.
[17] Will R, Englund R, Lubahn J, Cooney TE. Locking plates have increased torsional stiffness compared to standard plates in a segmental defect model of clavicle fracture. Arch Orthop Trauma Surg 2011; 131: 841-847.
[18] Blecha LD, Zambelli PY, Ramaniraka NA, Bourban PE, Månson JA, Pioletti DP. How plate positioning impacts the biomechanics of the open wedge tibial osteotomy; a finite element analysis. Comput Methods Biomech Biomed Engin 2005; 8: 307-313.
[19] Krishna KR, Sridhar I, Ghista DN. Analysis of the helical plate for bone fracture fixation. Injury 2008; 39: 1421-1436.
[20] Haller JM, O'Toole R, Graves M, Barei D, Gardner M, Kubiak E, Nascone J, Nork S, Presson AP, Higgins TF. How much articular displacement can be detected using fluoroscopy for tibial plateau fractures? Injury 2015; 46: 2243-2247.